Supplementary information for

Cis-clustering of cadherin-23 controls the kinetics of cell-cell adhesion

Cheerneni Sai Srinivas[1#], Gayathri Sindhuri Singaraju[1#], Nisha Arora[1], Sayan Das[1], Amin Sagar[1], Anuj Kumar[2],and Sabyasachi Rakshit[1,3*]

[*]Correspondence to Sabyasachi Rakshit: srakshit@iisermohali.ac.in

[#] Equal contributions

This PDF includes:

Supplimentary Figures:

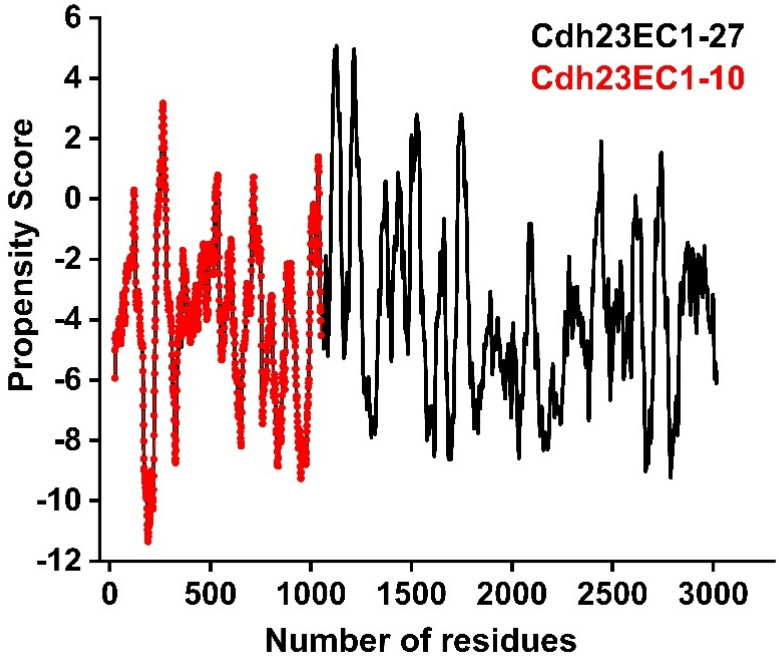

Figure S1. The high propensity of Cdh23 EC1-27 to undergo liquid-liquid phase-separation than Cdh23 EC1-10. The plot of the propensity scores estimated using catGRANULE algorithm for Cdh23 EC1-27(black) and Cdh23 EC1-10(red) versus the number of residues shows that a higher number of EC domains is having a higher probability of undergoing LLPS. Propensity scores for Cdh23 EC1-27 and Cdh23 EC1-10 are 1.2932 and 0.8012, respectively.

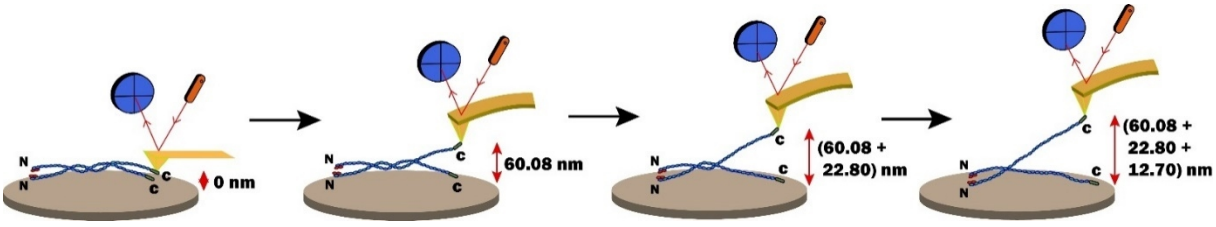

Figure S2. Schematic representation of the rupturing of cis-dimers from single-molecule pulling using AFM (Supporting to Fig. 1 A and B). Cartoon representation showing different steps of cis-dimer rupture upon retraction of AFM cantilever. After cis-dimer formation, when the cantilever is retracted, an average entropic extension of 60.1 nm is observed, followed by breaking (unzipping) of two cis-dimeric interactions leading toextensions of 22.8±0.4 nm and 12.7±0.8 nm, respectively. The overall extension on average is 60.1+22.8+12.7 nm. Further, more retraction would break the final interaction and release the cantilever.

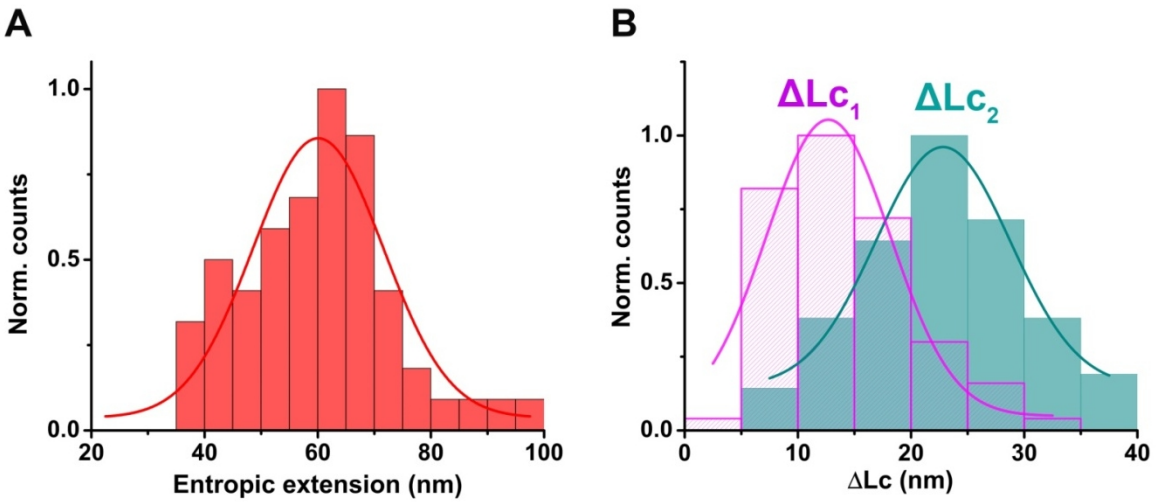

Figure S3. Contour length distributions of Cdh23 cis-dimer (Supporting to Fig. 1 B). Rupturing of Cdh23 cis-dimers by single-molecule pulling using AFM features three unbinding patterns, an entropic extension followed by two unzippings. The distribution of the entropic extension of the cis-dimers upon rupturing is shown in (**A**) with peak maxima at 60.1±1.3 nm. The solid line is a Gaussian fit to the histogram. **(B)** Histograms of the contour length changes associated with unzipping, ΔLc_1 (Magenta) and ΔLc_2 (Green), estimated from the WLC fitting of the force-extension curves. Solid lines are corresponding Gaussian fits. The peak-maxima for ΔLc_1 is 22.8±0.4 nm and for ΔLc_2 is 12.7±0.8 nm.

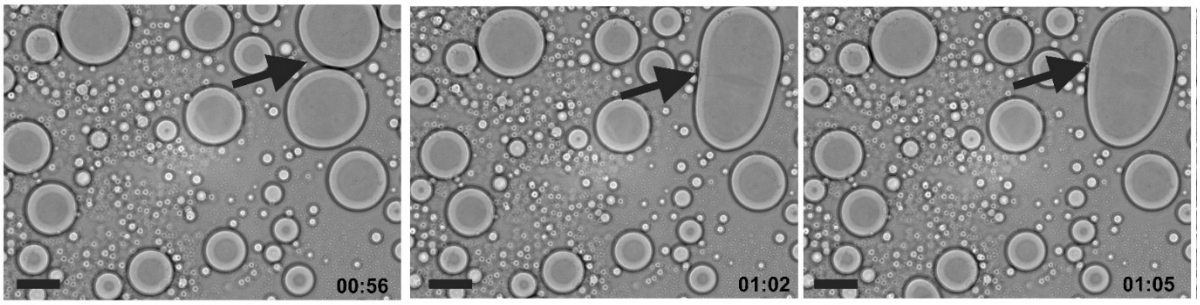

Figure S4. Time-lapse images of droplet fusion (Supporting to Fig. 1, E and F). The bright-field images with time capture one of the fusion events of liquid droplets of Cdh23 EC1-27. Arrows in black are highlighting the droplets undergoing fusion. Scale bar: 50 μm.

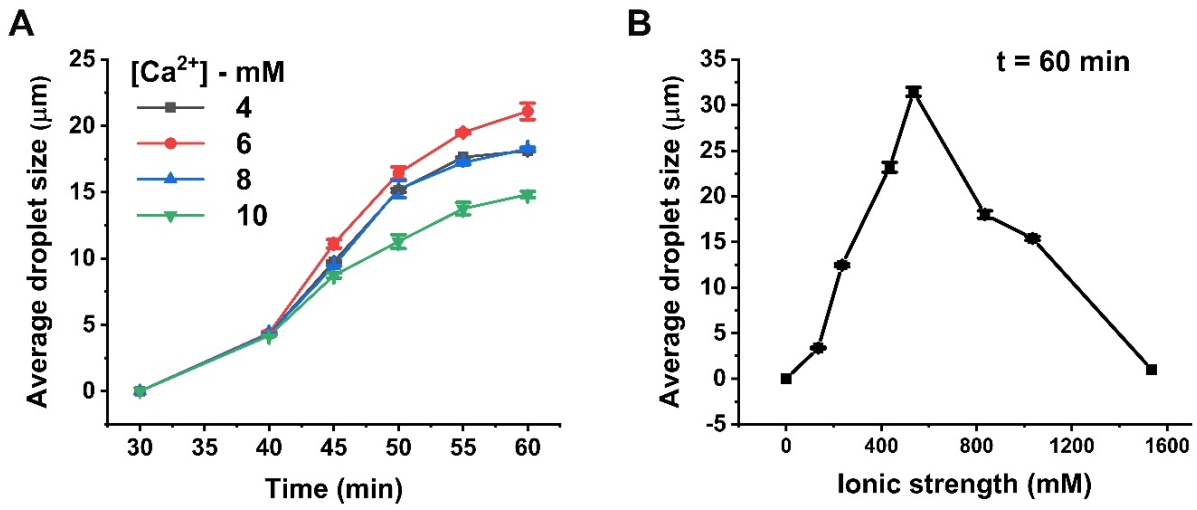

Figure S5. Systematic alterations of Ca^{2+} ions for the optimization of LLPS of Cdh23 EC1-27 (Supporting to Fig. 1, G, H and I). (A) The growth of liquid droplets (μm) of Cdh23 EC1-27 with time depends on Ca^{2+} concentration. Error bars represent the standard error of the mean (SEM) for N=30 droplets. **(B)** The liquid droplet size of Cdh23 EC1-27 measured after 60 min of nucleation follows a typical bell-shaped curve with increasing ionic strength of the buffer. Error bars represent SEM with N=30 droplets.

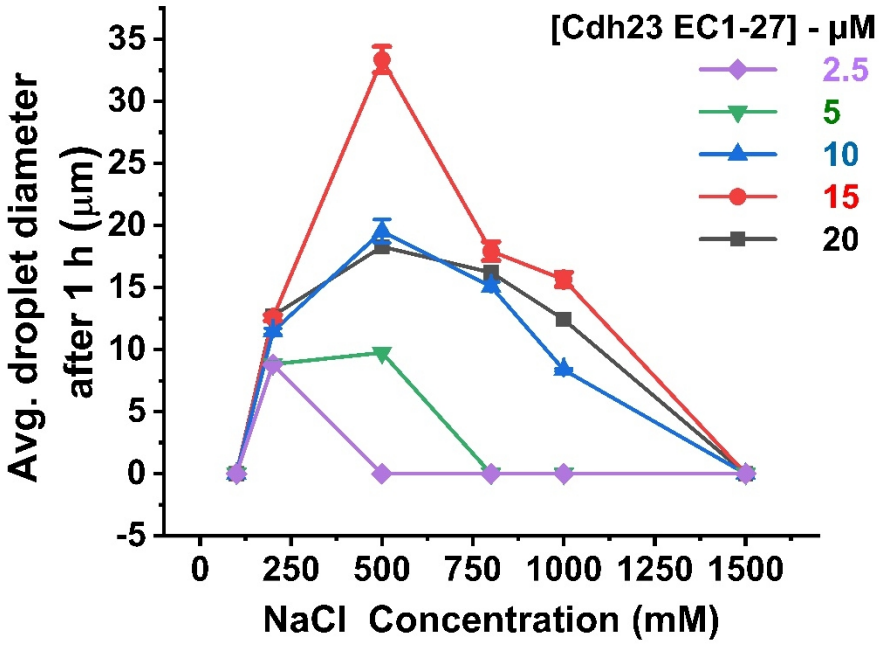

Figure S6. Optimization of LLPS of Cdh23 EC1-27 at varying NaCl and protein concentrations (Supporting to Fig. 1 H). Error bars represent SEM with N=30 droplets.

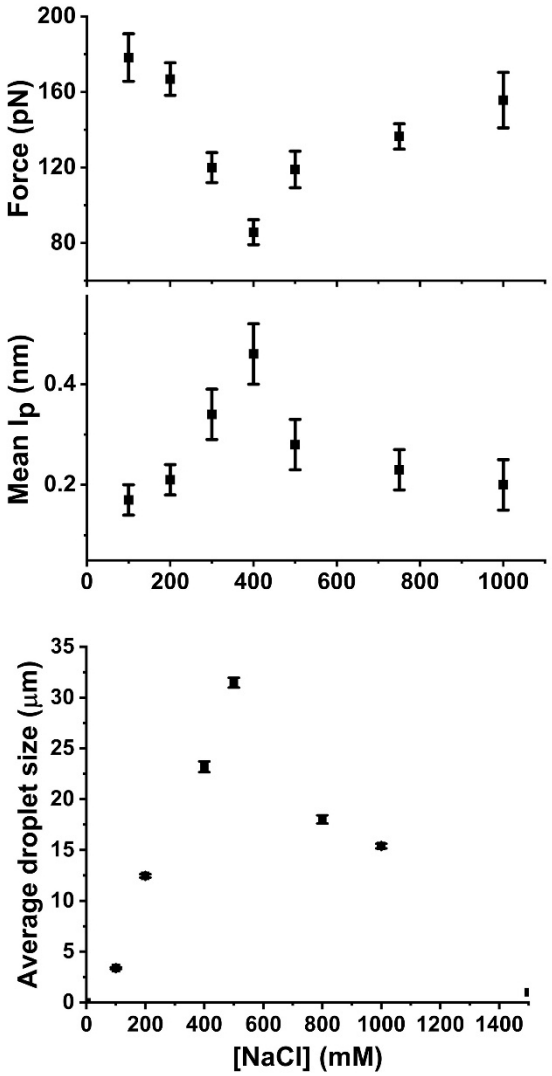

Figure S7. Correlation between cis-dimer's persistence length and resilience with the liquid droplets of Cdh23 EC1-27 with varying NaCl concentrations (Supporting to Fig. 1 I). A comparative plot depicting the trend in the persistence length and resilience of cis-interactions and droplets of Cdh23 EC1-27 with increasing NaCl. The overlay figures highlight a correlation of persistence length of the cis-interactions with the droplet size, while converse relation of droplet size with the strength of cis-interactions at varying ionic strength of the measuring buffer. The error bars in the upper panel are the standard error of Gaussian fitting of force histograms. Error bars in the middle panel and bottom panel represent SEM.

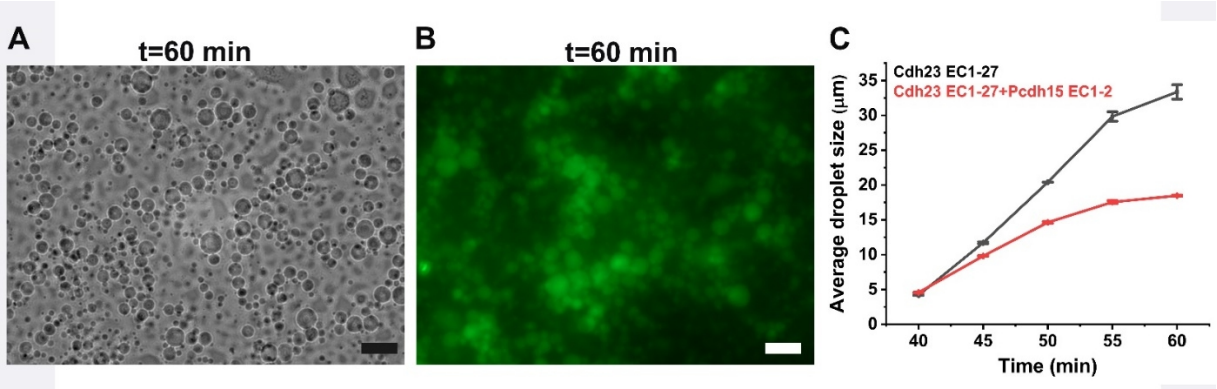

Figure S8. LLPS of Cdh23 EC1-27 in the absence of trans-interactions. (A) Bright-field and **(B)** fluorescence images of liquid droplets of Cdh23 EC1-27 induced by exclusive cis-interactions. The trans-interactions were turned off by introducing Pcdh15 EC1-2 in the buffer. The scale bar is 50 µm. **(C)** The comparative growth kinetics of liquid droplets (µm) of Cdh23 EC1-27 in the absence (black) and presence (red) of Pcdh15 EC1-2. Pcdh15 blocks the homophilic trans-binding interface of Cdh23.

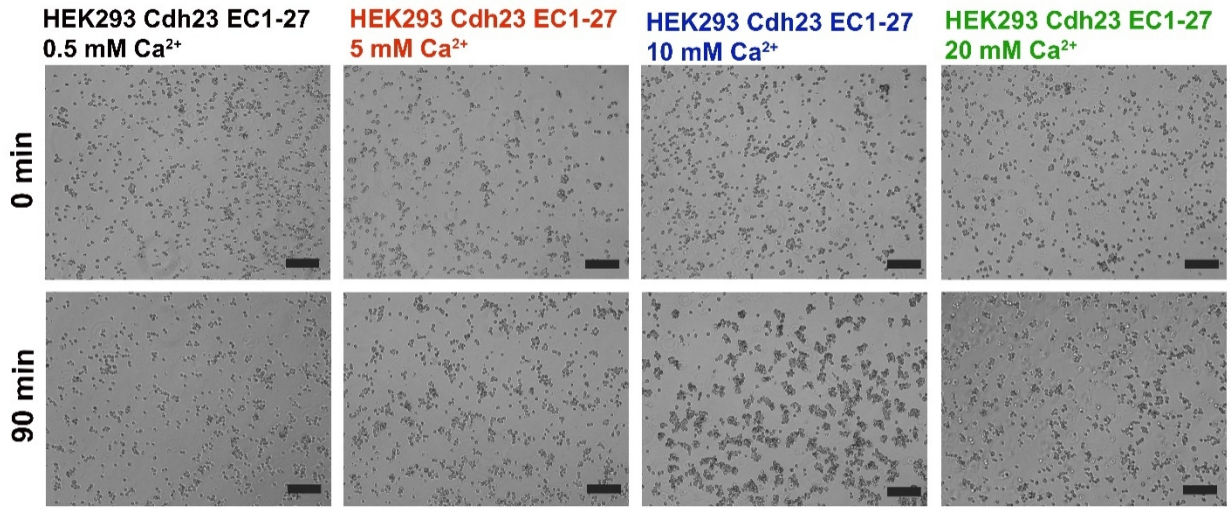

Figure S9. Calcium-dependent cell-cell aggregation of HEK293 cells exogenously expressing Cdh23 (Supporting to Fig. 2 D). Scale bar: 50 μm

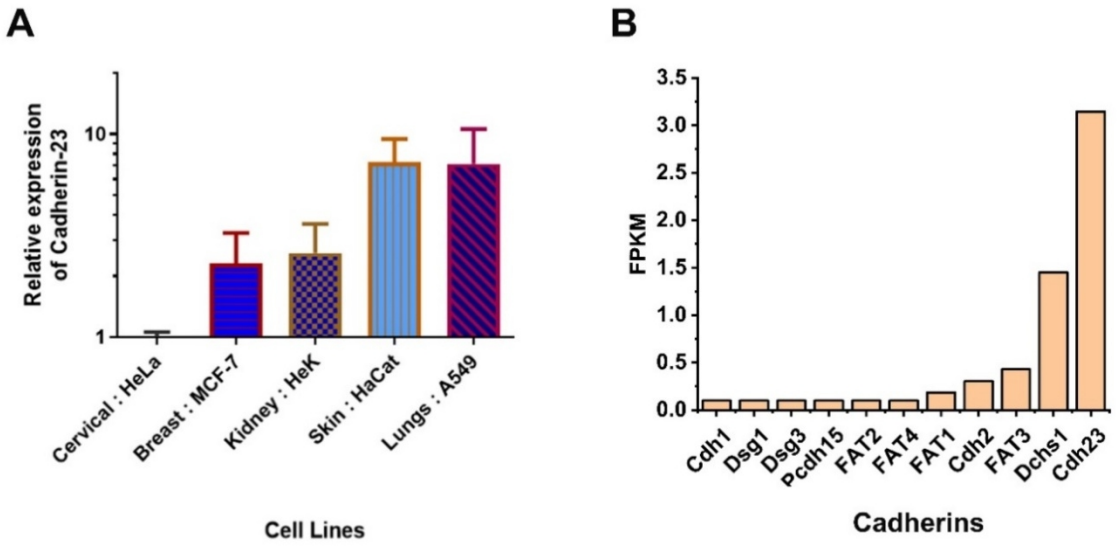

Figure S10. Differential expression of Cdh23 in cancer cell lines and microglia (Supporting to Fig. 3). (**A)** The relative expression of Cdh23 mRNA in different cancer cell lines, namely HeLa, MCF-7, HEK293, HaCat, and A549, quantified using qRT-PCR. The highest expression is noticed in A549 and the most negligible expression in HeLa. (**B)** Bar plot to display the mRNA expression of different cadherin proteins in microglia cells. FPKM is Fragments Per Kilobase Million essentially represents normalized expression values.

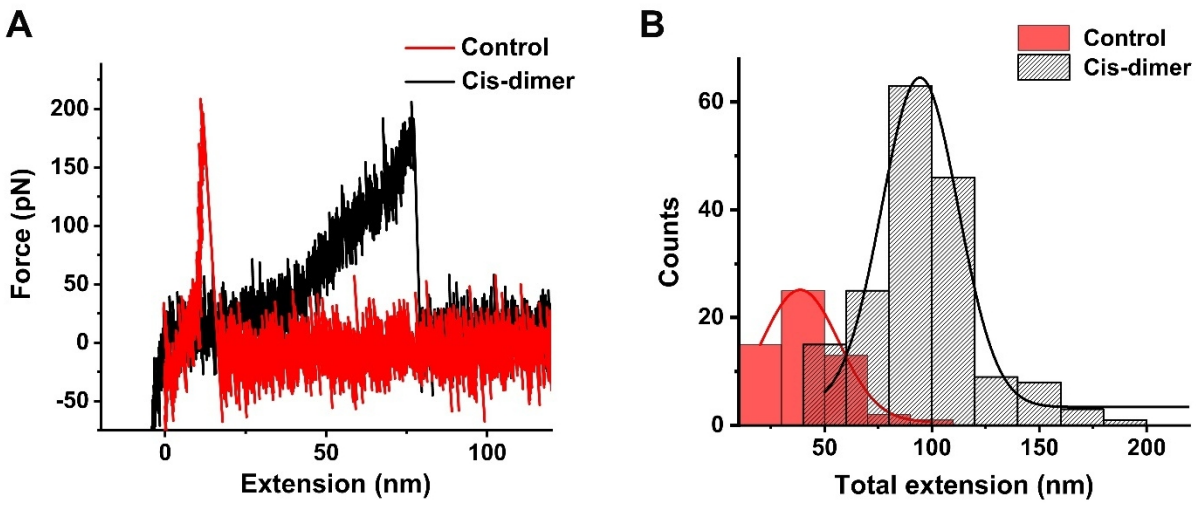

Figure S11. Validation of the specificity of single-molecule measurements of cis-dimer rupture using AFM. (A) Typical force-extension curves of specific (black) and control (non-specific) experiments **(B)** Distributions of the total extensions observed in control or non-specific (Red) and specific cis-dimer experiments (Black). Gaussian fitting of the histogram gives the mean extension of 38.7±0.5 nm in control and 94.4±1.4 nm in cis-dimer force-extension traces. Based on extension-distributions for non-specific force-extension measurements, we filtered out curves or events from the specific events before analyzing kinetic parameters for cis-interactions.

Video 1 A. Fusion of droplets of Cdh23 EC1-27 (Supporting to Fig. 1 F). The fusion of liquid droplets of Cdh23 EC1-27 captured under a fluorescence (GFP) microscope.

Video 1 B. Fusion of droplets of Cdh23 EC1-27 (Supporting to Fig. 1 E). The fusion of liquid droplets of Cdh23 EC1-27 captured under bright-field.

Table S1. The value of γ obtained from the fitting of the cell aggregation kinetics to Von Bertalanffy model.

Cell aggregation experiment	γ
Cdh23 EC1-10 and Cdh23 EC1-27	-2.25
Cdh23 EC1-27 at different Ca^{2+} concentrations	

γ represents the growth of the aggregate.

-